Journal of Computational Physics 229 (2010) 2659–2674

Contents lists available at ScienceDirect

Journal of Computational Physics

journal homepage: www.elsevier.com/locate/jcp

Diffusion front capturing schemes for a class of Fokker–Planck equations: Application to the relativistic heat equation

Antonio Marquina *

Departmento de Matematica Aplicada, Universidad de Valencia, Avda. Dr. Moliner 50, Burjassot-Valencia 46100, Spain

ARTICLE INFO

Article history:
Received 3 September 2009
Received in revised form 18 November 2009
Accepted 8 December 2009
Available online 16 December 2009

Dedicated to the memory of Fuensanta Andreu.

Keywords:
Diffusion fronts
Fokker–Planck equation
Relativistic heat equation
Conservative finite difference scheme

ABSTRACT

In this research work we introduce and analyze an explicit conservative finite difference scheme to approximate the solution of initial-boundary value problems for a class of limited diffusion Fokker–Planck equations under homogeneous Neumann boundary conditions. We show stability and positivity preserving property under a Courant–Friedrichs–Lewy parabolic time step restriction. We focus on the relativistic heat equation as a model problem of the mentioned limited diffusion Fokker–Planck equations. We analyze its dynamics and observe the presence of a singular flux and an implicit combination of nonlinear effects that include anisotropic diffusion and hyperbolic transport. We present numerical approximations of the solution of the relativistic heat equation for a set of examples in one and two dimensions including continuous initial data that develops jump discontinuities in finite time. We perform the numerical experiments through a class of explicit high order accurate conservative and stable numerical schemes and a semi-implicit nonlinear Crank–Nicolson type scheme.

1. Introduction

Numerical approximations to the solution of continuum physical models allow to better understand the behavior of their dynamics when analytical solutions are not available. In this paper we propose a conservative numerical scheme to approximate the solution of initial-boundary value problems for a class of limited diffusion Fokker–Planck equations.

The classical Fokker–Planck formulation [24,32] describes the transport of a physical magnitude $u \geqslant 0$ in a continuum medium and can be understood as an extension of the classical theory of heat conduction by Fourier [16]. The general form of the Fokker–Planck equation is expressed as

$$u_t = \nabla(g(u)\nabla u) \quad t > 0 \; g(u) > 0 \tag{1}$$

This equation represents the continuum model of many complex physical systems. Some examples include porous media equations, plasma equation, radiative transfer, image denoising by anisotropic diffusion and phenomena ruled by diffusion transfer in anisotropic media [5,7,11,15,22,24,25,27,32,34,35]. Processes described by this equation are related to transport by (anisotropic) diffusion where $g(u) > 0$ represents the diffusion coefficient. Several authors have pointed out that the infinite speed of propagation prescribed by Fourier theory of heat conduction is not appropriate for the description of the transport of many dissipative processes in thermodynamics and heat transfer [10,18,20,25,26]. The main limitation associated to the general model is that its solution does not contain diffusion fronts moving with finite speed. This issue has been a subject

* Tel.: +34 96354 4358; fax: +34 96354 3922.
E-mail address: antonio.marquina@uv.es.

0021-9991/$ - see front matter © 2009 Elsevier Inc. All rights reserved.
doi:10.1016/j.jcp.2009.12.014

of wide discussion and research during the last fifty years with well founded attempts to correct it and overcome its limitations [10,18,20,26].

Rosenau in [26] is the first one propounding satisfactory premises for a model for heat conduction consistent with the theory of special relativity in which the flux saturates as gradients tend to infinity. He proposes a generalized Fokker–Planck equation of the form

$$u_t = \nabla f(u, \nabla u) \tag{2}$$

that overcomes the limitations of (1). The solution to this equation allows diffusion fronts propagating at a prescribed finite speed. Rosenau model was subsequently named relativistic heat equation [6,8,19,35,34] .

The relativistic heat equation represents a mathematical model describing the transport by diffusion with finite speed of propagation. The diffusion of relativistic heat equation is confined to a region limited by a front that propagates at the speed of light. Theory of existence and uniqueness of the solution of the relativistic heat equation has been proved by Andreu and collaborators in [1,2,4,5] as a particular case of a generalized class of the Fokker–Planck equations. These authors develop a mathematical theory of the entropy solutions associated to (2).

The main goal of this research work consists of understanding better the dynamics of the physical processes described by the relativistic heat equation through numerical approximations. To that end we design a reliable conservative numerical scheme to approximate the solution of a wide class of Fokker–Planck equations that are able to describe transport phenomena containing propagating fronts moving with finite speed. This class of limited diffusion equations includes the relativistic heat equation as a significant model example.

In this paper we propose a conservative numerical scheme to approximate the solution of a wide class of Fokker–Planck equations and prove that the numerical scheme preserves positivity, satisfies a discrete local maximum principle and is stable under a Courant–Friedrichs–Lewy parabolic time step restriction [12,21]. We focus on the numerical approximation of the relativistic heat equation which is a significant model example of the mentioned generalized class of limited diffusion equations. We analyze the dynamics of the relativistic heat equation and observe the presence of a singular flux and an implicit combination of nonlinear effects that include anisotropic diffusion and hyperbolic transport. We then approximate the solution of a set of examples for the relativistic heat equation through a class of explicit high order accurate conservative and stable numerical schemes and a semi-implicit nonlinear Crank–Nicolson type scheme that improves computational efficiency over the explicit ones.

The paper is organized as follows. In Section 2 we present a heuristic approach on the relativistic heat equation. Section 3 is devoted to propose and analyze an explicit conservative numerical scheme to approximate the solution of the generalized class of Fokker–Planck equations. In Section 4 we provide one- and two-dimensional explicit numerical schemes to approximate the solution of the relativistic heat equation and we formulate a semi-implicit nonlinear Crank–Nicolson type numerical scheme to relax the Courant–Friedrichs–Lewy parabolic restriction. Section 5 includes the formulation for high order accurate implementations of the scheme and a set of numerical tests for the relativistic heat equation in one and two dimensions. In Section 6 we draw our conclusions.

2. A heuristic approach to the relativistic heat equation

The heat equation was proposed by Fourier as a mathematical model to describe heat conduction. The equation reads as

$$u_t = v\Delta u \tag{3}$$

where u represents the temperature distribution and $v > 0$ is the coefficient of heat diffusion in a specific media. Eq. (3) represents the simplest case of a Fokker–Planck equation Eq. (1) with $g(u) = v$. When the initial data for the heat equation is a punctual impulse of heat (represented by a delta function) the solution of the equation at every time $t > 0$ is a Gaussian distribution centered at the point where the heat impulse is applied. This property on the solution of (3) implies that the speed of heat propagation is infinite.

We can express Eq. (3) in conservation form as

$$u_t + \nabla\left(-uv\frac{\nabla u}{u}\right) = 0 \tag{4}$$

where

$$-uv\frac{\nabla u}{u} \tag{5}$$

represents the heat flux defined as the conserved variable multiplied by the flow velocity. The velocity field

$$\vec{v} = -v\frac{\nabla u}{u} \tag{6}$$

is proportional to the possibly unbounded gradient of u and therefore the velocity of heat transfer $\vec{v}$ in (4) is not limited.

Rosenau proposes to use a different velocity field $\vec{v}_R$ instead of $\vec{v}$ in (4) to enforce the magnitude of the velocity field not to exceed the speed of light $c > 0$. Then the modified heat equation

$$u_t + \nabla(u\vec{v}_R) = 0 \tag{7}$$

would approach classical heat equation (4) for small $|\vec{v}_R|$ and propagate the solution with limited speed for large $|\vec{v}_R|$.

To this end $\vec{v}_R$ is defined from $\vec{v}$ by weightening $\vec{v}_R$ with the dimensionless Lorentz factor $W = \frac{1}{\sqrt{1-\frac{|\vec{v}_R|^2}{c^2}}}$ such that

$$\frac{\vec{v}_R}{\sqrt{1-\frac{|\vec{v}_R|^2}{c^2}}} = \vec{v} \tag{8}$$

To determine an explicit expression of $\vec{v}_R$ let us proceed as follows. Let $\vec{n} = \frac{\vec{v}}{|\vec{v}|}$ be the unit vector of $\vec{v}$. Then

$$\vec{v}_R = \vec{n}|\vec{v}_R| \tag{9}$$

We can get $|\vec{v}_R|$ from (8) by calculating the square of the magnitude of $\vec{v}$

$$\vec{v}\cdot\vec{v} = |\vec{v}|^2 = \frac{|\vec{v}_R|^2}{1-\frac{|\vec{v}_R|^2}{c^2}} \tag{10}$$

and from this we obtain

$$|\vec{v}_R| = \frac{|\vec{v}|}{\sqrt{1+\frac{|\vec{v}|^2}{c^2}}} \tag{11}$$

Thus, from (9)

$$\vec{v}_R = \vec{n}|\vec{v}_R| = \frac{\vec{v}}{|\vec{v}|}\frac{|\vec{v}|}{\sqrt{1+\frac{|\vec{v}|^2}{c^2}}} = \frac{\vec{v}}{1+\frac{|\vec{v}|^2}{c^2}} \tag{12}$$

Therefore, using (6) we obtain

$$\vec{v}_R = -\frac{v\nabla u}{u\sqrt{1+\left(\frac{v}{c}\frac{|\nabla u|}{u}\right)^2}} = -\frac{v\nabla u}{\sqrt{u^2+\left(\frac{v}{c}|\nabla u|\right)^2}} \tag{13}$$

The resulting equation with the new flux $f_R = u\vec{v}_R$ is the relativistic heat equation

$$u_t = \nabla\left(\frac{vu\nabla u}{\sqrt{u^2+\left(\frac{v}{c}\right)^2|\nabla u|^2}}\right) \tag{14}$$

Let us observe that in the case that c is a parameter such that $c \to +\infty$, Eq. (14) tends to the classical heat equation [9]. Moreover, (as proved in [4]) if $v \to +\infty$, the relativistic heat equation tends to the transparent media diffusion equation

$$u_t = c\nabla\left(u\frac{\nabla u}{|\nabla u|}\right) \tag{15}$$

Andreu et al. in [1–5] have performed an extended analytical study on the relativistic heat equation and its solution for a particular class of initial data. However there are not at the moment explicit solutions of the relativistic heat equation.

Our goal is to propose a consistent and stable numerical scheme to approximate the solution of the relativistic heat equation and be able to study a wide class of initial-boundary value problems. To tackle this goal we first develop a heuristic analysis to better understand the dynamics of the solution of the relativistic heat conduction model.

The one-dimensional relativistic heat equation can be expressed as

$$u_t = v\left(\frac{uu_x}{\sqrt{u^2+r^2u_x^2}}\right)_x, \quad t>0,\ u \geqslant 0 \tag{16}$$

where $v>0$ and $r=\frac{v}{c}$.

Expanding spatial derivatives of the flux we observe that (16) can be expressed as

$$u_t = c\left(\frac{ru_x}{\sqrt{u^2+r^2u_x^2}}\right)^3 u_x + v\left(\frac{u}{\sqrt{u^2+r^2u_x^2}}\right)^3 u_{xx} \tag{17}$$

which represents the relativistic heat equation splitted into two terms, a Hamilton–Jacobi term that depends on u and its derivative and a diffusive type term, respectively. The Hamilton–Jacobi term

$$c\left(\frac{ru_x}{\sqrt{u^2+r^2u_x^2}}\right)^3 u_x \tag{18}$$

depends on u in a nonstandard way from the point of view of classical theory of viscosity solutions. Hamiltonians of classical Hamilton–Jacobi equations are non-decreasing functions on u and their solutions are continuous and develop rarefactions and discontinuities only in derivative (kinks) [13]. Recently, Giga in [17] extends classical theory on viscosity solution for Hamilton–Jacobi equations to the case where the Hamiltonian is a non-increasing function of u. In this case he proves that the solution might develop not only rarefactions and kinks but jump discontinuities (shocks) in finite time.

We focus on the Hamiltonian (18) that is a non-increasing function of u and from the following analysis we observe that it resembles a hyperbolic advection equation around discontinuities.

Let us consider the Hamilton–Jacobi equation

$$u_t = c\left(\frac{ru_x}{\sqrt{u^2 + r^2u_x^2}}\right)^3 u_x \tag{19}$$

Around jump discontinuities or "large gradients" where $|u_x| \gg u$, the ratio $\frac{u}{r|u_x|} \ll 1$ is small and we can re-write Eq. (19) as

$$u_t = c\left(\frac{\frac{ru_x}{r|u_x|}}{\sqrt{\left(\frac{u}{ru_x}\right)^2 + 1}}\right)^3 u_x \tag{20}$$

and defining $\operatorname{sgn}(u_x) = \frac{u_x}{|u_x|}$ we obtain

$$u_t = c\frac{\operatorname{sgn}(u_x)}{\left(\sqrt{\left(\frac{u}{ru_x}\right)^2 + 1}\right)^3} u_x \tag{21}$$

We can express this equation using the Taylor expansion of $(1+y)^{-\frac{3}{2}} = 1 - \frac{3}{2}y + \frac{15}{8}y^2 + O(y^3)$ (convergent for $|y| < 1$) for $y = \frac{u}{ru_x}$ as,

$$u_t = c\operatorname{sgn}(u_x)\left(1 - \frac{3}{2}\left(\frac{u}{ru_x}\right)^2 + \frac{15}{8}\left(\frac{u}{ru_x}\right)^4 - \cdots\right)u_x \tag{22}$$

Then, assuming $\frac{u}{r|u_x|} \ll 1$ the above equation approaches to

$$u_t \approx c\operatorname{sgn}(u_x)u_x \tag{23}$$

which is a linear advection.

Eq. (19) approaches linear Eq. (23) around jump discontinuities and propagates them at speed $c > 0$ according to the direction prescribed by the sign of u_x. Thus the non-classical Hamilton–Jacobi term in (17) is a convective term that will be responsible of the development of waves, kinks and shocks in the solution where shocks will not propagate faster than the speed of light c. This argument is consistent with the results and theory proposed by Giga in [17].

Similarly in two dimensions we can obtain the splitted form of the relativistic heat equation as

$$u_t = \frac{vr^2|\nabla u|^4}{(u^2 + r^2|\nabla u|^2)^{\frac{3}{2}}} + \frac{vu}{(u^2 + r^2|\nabla u|^2)^{\frac{3}{2}}}\left((u^2 + r^2u_y^2)u_{xx} - 2r^2u_xu_yu_{xy} + (u^2 + r^2u_x^2)u_{yy}\right) \tag{24}$$

where $r = \frac{v}{c}$.

This equation is parabolic when u is non-negative and has a singularity for $u = 0$ and $|\nabla u| = 0$.

Expression (24) contains the hyperbolic term

$$\frac{vr^2|\nabla u|^4}{(u^2 + r^2|\nabla u|^2)^{\frac{3}{2}}} \tag{25}$$

which is responsible for the finite speed of propagation of jump discontinuities. Indeed considering Eq. (24) removing the second order term we get the Hamilton–Jacobi equation

$$u_t = c\left[\frac{r|\nabla u|}{(u^2 + r^2|\nabla u|^2)^{\frac{1}{2}}}\right]^3 |\nabla u| \tag{26}$$

that belongs to a class of Hamilton–Jacobi equations which viscosity solutions contain kinks, rarefactions waves and shocks (see [17]).

We observe that as time evolves in (17) and (24) the effects of the parabolic terms might diffuse possible present shocks. However at the boundary of the support of u where $u \approx 0$ the local anisotropic diffusion vanishes and Eqs. (17) and (24) might develop propagating shocks called "diffusion fronts" that expand the support of the solution.

It has been proved by Andreu et al. [1,2,4,5] that in the case that the initial data of the relativistic heat equation is a function of compact support there exists an entropy solution that contains "diffusion fronts" that propagate at speed c.

In the next section we will design a numerical scheme to approximate the solution of the class of Fokker–Planck equations that are able to capture diffusion fronts when they are present in the solution as in the case of the relativistic heat equation.

3. Conservative finite difference schemes for a class of limited diffusion equations

In this section we propose a conservative finite difference numerical scheme that approximates the solution of a class of Fokker–Planck limited diffusion equations to which the relativistic heat equation is a particular case. The explicit numerical scheme is consistent and stable under a parabolic type Courant–Friedrichs–Lewy restriction on the time step [12]. The scheme conserves mass exactly, preserves positivity and satisfies a discrete local maximum principle. In addition we propose nonlinear Crank–Nicolson implicit and semi-implicit versions of the scheme that relax the parabolic Courant–Friedrichs–Lewy restriction improving computational efficiency.

Let us consider the generalized Fokker–Planck equation in m spatial dimensions

$$u_t = \nabla \cdot \mathbf{f}(u, \nabla u), \quad t > 0 \tag{27}$$

where $x = (x^{(1)}, \ldots, x^{(m)})$ and $u(x,t)$ is defined for $x \in D = [a,b]^m,\ a < b,\ f = (f^{(1)}, \ldots, f^{(m)})$.

We impose the initial data

$$u(x,0) = u_0(x), \quad x \in D \tag{28}$$

under homogeneous Neumann boundary conditions,

$$\frac{\partial u(x,t)}{\partial x^{(i)}} = 0, \quad x \in \partial D \text{ and } t > 0\ 1 \leqslant i \leqslant m \tag{29}$$

We express (27) in explicit partial derivatives

$$u_t = \sum_{i=1}^{m} \frac{\partial}{\partial x^{(i)}} \left[f^{(i)}(u(x,t), \nabla u(x,t)) \right] \tag{30}$$

where

$$\nabla u(x,t) = \left(\frac{\partial u}{\partial x^{(1)}}, \frac{\partial u}{\partial x^{(2)}}, \ldots, \frac{\partial u}{\partial x^{(m)}} \right) \tag{31}$$

We set the computational domain as follows. We consider a uniform mesh on D defined from a partition of $[a,b]$ in N subintervals of length $h = \frac{b-a}{N}$. Let us define the vector of indices $j = (j_1, j_2, \cdots, j_m)^T$. Then, the nodes of the grid are defined by

$$x_j = \left(x_{j_1}^{(1)}, \ldots, x_{j_m}^{(m)} \right) \tag{32}$$

where $1 \leqslant j_k \leqslant N$ and $x_{j_k}^{(k)} := a + j_k h$.

Next let us introduce the concept of conservative numerical scheme associated to (30).

We denote by u_j^n the numerical approximation of the solution of (27), $u(x_j, t_n)$ where x_j is defined as (32) and $t_n = n\Delta t,\ \Delta t > 0$ the time step size.

Definition 1. A first order accurate conservative finite difference scheme in m dimensions for solving (30) reads as

$$u_j^{n+1} = u_j^n + \frac{\Delta t}{h} \sum_{i=1}^{m} \left[\tilde{f}^{(i)}_{j+\frac{e_i}{2}} - \tilde{f}^{(i)}_{j-\frac{e_i}{2}} \right] \tag{33}$$

where $j = (j_1, j_2, \ldots, j_m)$ is a fixed coordinate location, $e_i \in \mathscr{R}^m$ is the unit vector $e_i(k) = \delta_{ik}$ and $\tilde{f}^{(i)}_{j+\frac{e_i}{2}}$ is a scalar numerical flux defined as a function of the variables

$$\tilde{f}^{(i)}_{j+\frac{e_i}{2}} = \tilde{f}^{(i)}_{j+\frac{e_i}{2}} \left(u^n_{j-p_1 e_i}, \ldots, u^n_{j+q_1 e_i}; (\nabla u^{(i)})_{x_{j+\frac{e_i}{2}}} \right) \tag{34}$$

which is consistent with the flux in (30) in the direction of $e_i,\ f^{(i)}$, i.e.,

$$\tilde{f}^{(i)}_{j+\frac{e_i}{2}}(u, u, \ldots, u; w) = \tilde{f}^{(i)}(u, (w, \ldots, w)^T) \tag{35}$$

The term $(\nabla u^{(i)})_{x_{j+\frac{e_i}{2}}}$ is defined by a vector of first order divided differences in the direction e_i that approximates the partial derivatives at the location $x_{j+\frac{e_i}{2}}$

$$(\nabla u^{(i)})_{x_{j+\frac{e_i}{2}}} = (d_1, \ldots, d_i, \ldots, d_m) \tag{36}$$

where

$$d_i = \frac{u(x_{j+e_i}) - u(x_j)}{h} \tag{37}$$

and for $k \neq i$

$$d_k = \frac{1}{2h}\left[\frac{u(x_{j+e_k}) + u(x_{j+e_k+e_i})}{2} - \frac{u(x_{j-e_k}) + u(x_{j-e_k+e_i})}{2}\right] \tag{38}$$

Let us consider the class of Fokker–Planck equations as Eq. (30) with a flux of the form

$$f(u, \nabla u) := g(u, |\nabla u|)\nabla u \tag{39}$$

where the diffusion coefficient $g(z, w)$ is a non-negative real function of its arguments which is uniformly bounded, i.e., there is a constant $M > 0$ such that

$$g(z, w) \leqslant M, \quad \text{for all } z, w \tag{40}$$

This type of flux functions allow to define anisotropic diffusion equations with anomalous diffusion (depending on u and ∇u) [24,34,35].

Expression (30) for this family of fluxes reads as

$$u_t = \sum_{i=1}^{m} \frac{\partial}{\partial x^{(i)}}\left[g(u(x,t), |\nabla u(x,t)|)\frac{\partial u}{\partial x^{(i)}}\right] \tag{41}$$

where

$$|\nabla u(x,t)| = \left[\sum_{k=1}^{m}\left|\frac{\partial u(x,t)}{\partial x^{(k)}}\right|^2\right]^{\frac{1}{2}} \tag{42}$$

Next, to design a conservative finite difference scheme for Eq. (41), we define a consistent numerical flux satisfying (34) and (35) as

$$\tilde{f}^{(i)}_{j+\frac{e_i}{2}} = g\left(\frac{u_j + u_{j+e_i}}{2}, |\nabla u^{(i)}|_{j+\frac{e_i}{2}}\right)\frac{u_{j+e_i} - u_j}{h} \tag{43}$$

where

$$|\nabla u^{(i)}|_{x_{j+\frac{e_i}{2}}} = \left[d_i^2 + \sum_{k \neq i} d_k^2\right]^{\frac{1}{2}} \tag{44}$$

with d_i and d_k computed from expressions (37) and (38), respectively.

The complete numerical scheme reads as

$$u_j^{n+1} = u_j^n + \frac{\Delta t}{h^2}\sum_{i=1}^{m}\left[g\left(\frac{u_j + u_{j+e_i}}{2}, |\nabla u^{(i)}|_{x_{j+\frac{e_i}{2}}}\right)(u_{j+e_i} - u_j) - g\left(\frac{u_{j-e_i} + u_j}{2}, |\nabla u^{(i)}|_{x_{j-\frac{e_i}{2}}}\right)(u_j - u_{j-e_i})\right] \tag{45}$$

Theorem 1. *The conservative numerical scheme (45) associated to the Fokker–Planck equations as Eq. (41) satisfying (40) for some $M > 0$ has the following properties:*

(1) The scheme preserves positivity and is stable under the following Courant–Friedrichs–Lewy restriction on the time step

$$\frac{\Delta t}{h^2} \leqslant \frac{1}{2^m M} \tag{46}$$

(2) The numerical scheme satisfies a local maximum principle under condition (46), i.e., the magnitude of local maxima (local minima) does not increase (decrease) along time evolution.

Proof. We provide the proof for the case $m = 1$ and sketch how to extend it to any dimension m. The numerical scheme (45) for $m = 1$ can be written as

$$u_j^{n+1} = u_j^n + \frac{\Delta t}{h^2}\sum_{i=1}^{m}\left[g\left(\frac{u_j^n + ux_{j+1}^n}{2}, \left|\frac{u_{j+1}^n - u_j^n}{h}\right|\right)\left(u_{j+1}^n - u_j^n\right) - g\left(\frac{u_{j-1}^n + u_j^n}{2}, \left|\frac{u_j^n - u_{j-1}^n}{h}\right|\right)\left(u_j^n - u_{j-1}^n\right)\right] \tag{47}$$

Let us define

$$A(u_-, u_+) := g\left(\frac{u_- + u_+}{2}, \left|\frac{u_+ - u_-}{h}\right|\right) \tag{48}$$

We can write (47) in terms of A as

$$u_j^{n+1} = \frac{\Delta t}{h^2}A(u_{j-1}^n, u_j^n)u_{j-1}^n + \left[1 - \frac{\Delta t}{h^2}\left(A(u_{j-1}^n, u_j^n) + A(u_j^n, u_{j+1}^n)\right)\right]u_j^n + \frac{\Delta t}{h^2}A(u_j^n, u_{j+1}^n)u_{j+1}^n \tag{49}$$

In order to preserve positivity, we need to prove that $u_j^n \geqslant 0,\ \forall j$ implies $u_j^{n+1} \geqslant 0,\ \forall j$. Since $A(u_-, u_+) \geqslant 0$ for all u_-, u_+ and from (40) we have that $A(u_-, u_+) \leqslant M$ for all u_-, u_+ then, if Δt is chosen under restriction (46) the positivity is satisfied,

$$1 - \frac{\Delta t}{h^2}\left(A\left(u_{j-1}^n, u_j^n\right) + A\left(u_j^n, u_{j+1}^n\right)\right) \geqslant 1 - \frac{A\left(u_{j-1}^n, u_j^n\right) + A\left(u_j^n, u_{j+1}^n\right)}{2M} \geqslant 0 \tag{50}$$

Thus (46) ensures the property of positivity preserving.

In addition under restriction (46) each u_j^{n+1} is a nonlinear convex combination of u_{j-1}^n, u_j^n and u_{j+1}^n and therefore the scheme is stable and the local discrete maximum principle is satisfied.

The proof for $m > 1$ follows the same line of reasoning where the value of u_j^{n+1} is a convex combination of $2^m + 1$ terms, all coefficients are always non-negative except the ones corresponding to u_j^n. To enforce the positivity of the central coefficient it is enough that condition (46) is satisfied following the same argument as the one for $m = 1$.

The total mass of the computed solution from one time step to the next one is exactly conserved due to the telescoping cancellation obtained when calculating the sum of the u_j and the application of the homogeneous Neumann boundary conditions. □

We remark that the standard finite difference methods to approximate the solution to a general diffusion equation consists of using central differences in all derivatives present in the second order differential operator. However depending on the complexity of the diffusion operator not all of the schemes can be written in conservation form consistently with our Definition 1. An example of semidiscrete central difference scheme used in [11] for a particular one-dimensional diffusion equation can be proved to be conservative satisfying Definition 1.

Next we use the proposed numerical scheme to approximate the solution of the relativistic heat equation. The relativistic heat equation

$$u_t = v\left(\frac{u\nabla u}{\sqrt{u^2 + \left(\frac{v}{c}\right)^2 |\nabla u|^2}}\right) \tag{51}$$

belongs to the class of Eq. (41) with a flux g defined as

$$g_{\mathrm{RHE}}(z, w) = \frac{vz}{\sqrt{z^2 + r^2 w^2}} \tag{52}$$

where $v > 0$ and $r > 0$ are constants.

In the next section we propose explicit and implicit finite difference numerical schemes to approximate the solution of (51).

4. Finite difference numerical scheme for the approximation of the relativistic heat equation

In this section we propose finite difference schemes for the one- and two-dimensional relativistic heat equation that satisfy the properties described in Theorem 1 in the previous section.

4.1. One-dimensional numerical approximation of the relativistic heat equation

For computational purposes to avoid dividing by zero when $u_x = 0$ we consider a regularization of the one-dimensional relativistic heat equation consisting of adding a small constant $\epsilon > 0$ of the order of machine rounding error in the denominator of the flux. We will solve

$$u_t = v\left(\frac{uu_x}{\sqrt{u^2 + r^2 u_x^2 + \epsilon}}\right)_x, \quad t > 0,\ u \geqslant 0 \tag{53}$$

with initial data

$$u(x, 0) := u_0(x) \geqslant 0 \quad a \leqslant x \leqslant b \tag{54}$$

where $u_0(x)$ is of compact support in $]a, b[$ and homogeneous Neumann boundary conditions: $u_x(a, t) = u_x(b, t) = 0$.

The ϵ perturbation will not affect the accuracy of the numerical approximation since the double limit

$$\lim_{(\xi,\eta)\to(0,0)} \frac{\xi\eta}{\sqrt{\xi^2 + \eta^2}} = 0 \tag{55}$$

exists.

We consider the computational mesh defined for N number of subdivisions of the interval such that $h = \frac{b-a}{N}$ is the spatial step size and $x_j = a + jh,\ j = 0, 1, \ldots, N$. We denote by $t_n = n\Delta t,\ n \geqslant 0$ where $\Delta t > 0$ is the time step size.

The numerical scheme for the approximation of the one-dimensional relativistic heat equation, Eq. (53), will read as follows:

$$u_j^{n+1} = \frac{\Delta t}{h^2} A(u_{j-1}^n, u_j^n) u_{j-1}^n + \left[1 - \frac{\Delta t}{h^2}\left(A(u_{j-1}^n, u_j^n) + A(u_j^n, u_{j+1}^n)\right)\right] u_j^n + \frac{\Delta t}{h^2} A(u_j^n, u_{j+1}^n) u_{j+1}^n \tag{56}$$

where

$$A(u_j^n, u_{j+1}^n) = \frac{\frac{v}{2}(u_j^n + u_{j+1}^n)}{\sqrt{\left(\frac{u_j^n + u_{j+1}^n}{2}\right)^2 + r^2\left(\frac{u_{j+1}^n - u_j^n}{h}\right)^2 + \epsilon}} \tag{57}$$

and $\frac{\Delta t}{h^2} \leqslant \frac{1}{2v}$ to satisfy condition (46) in Theorem 1.

To relax the Courant–Friedrichs–Lewy time step restriction we can use a fully implicit Crank–Nicolson scheme [14] or a semi-implicit one, both second order accurate in space and time.

Let $a_j^n = A(u_j^n, u_{j+1}^n)$. The fully implicit Crank–Nicolson scheme will read as follows. Solve u_j^{n+1} from the nonlinear system of equations

$$\begin{aligned} &-\frac{1}{2}\frac{\Delta t}{h^2} a_{j-1}^{n+1} u_{j-1}^{n+1} + \left(1 + \frac{1}{2}\frac{\Delta t}{h^2}\left(a_{j-1}^{n+1} + a_j^{n+1}\right)\right) u_j^{n+1} - \frac{1}{2}\frac{\Delta t}{h^2} a_j^{n+1} u_{j+1}^{n+1} \\ &= \frac{1}{2}\frac{\Delta t}{h^2} a_{j-1}^n u_{j-1}^n + \left(1 - \frac{1}{2}\frac{\Delta t}{h^2}\left(a_{j-1}^n + a_j^n\right)\right) u_j^n + \frac{1}{2}\frac{\Delta t}{h^2} a_j^n u_{j+1}^n \end{aligned} \tag{58}$$

for $j = 1, 2, \ldots, N-1$, and $u_0^{n+1} = u_1^{n+1}$ and $u_N^{n+1} = u_{N-1}^{n+1}$ for the homogeneous Neumann boundary conditions.

The nonlinear system (58) can be solved by using a nonlinear Gauss–Seidel procedure that converges since the iteration matrix function has spectral radius strictly less than one [33].

A semi-implicit Crank–Nicolson scheme can be formulated by using $a_{j-1}^n,\ a_j^n$ and a_{j+1}^n as nonlinear coefficients on the left hand side of (58) instead of $a_{j-1}^{n+1},\ a_j^{n+1}$ and a_{j+1}^{n+1}. The resulting scheme is significantly more efficient since the nonlinear coefficients are computed once in every time step. Let us remark that the matrix of the linear system is not symmetric but it is diagonally dominant and therefore the convergence of the Gauss-Seidel iterative method is ensured. We have found through our numerical experiments that the semi-implicit Crank–Nicolson scheme becomes stable for $\Delta t = O(h)$.

4.2. Two-dimensional numerical approximation of the relativistic heat equation

We consider the initial-boundary value problem for the two-dimensional relativistic heat equation

$$u_t = v\frac{\partial}{\partial x}\left(\frac{u u_x}{[u^2 + r^2(u_x^2 + u_y^2) + \epsilon]^{\frac{1}{2}}}\right) + v\frac{\partial}{\partial y}\left(\frac{u u_y}{[u^2 + r^2(u_x^2 + u_y^2) + \epsilon]^{\frac{1}{2}}}\right) \tag{59}$$

for $t > 0,\ a \leqslant x,\ y \leqslant b$ with the initial data

$$u(x, y, 0) = u_0(x, y) \quad a \leqslant x,\ y \leqslant b \tag{60}$$

of compact support and homogeneous Neumann boundary conditions

$$u_x(a, y, t) = u_x(b, y, t) = u_y(x, a, t) = u_y(x, b, t) = 0 \tag{61}$$

We will use a uniform grid with $\Delta x = \Delta y = h > 0$ with $h = \frac{b-a}{N}$ with N the number of subdivisions of the computational domain. We define $x_j := a + jh, j = 0, \ldots, N$ and $y_k := a + kh, k = 0, \ldots, N$. We denote by $t_n = n\Delta t$ where $\Delta t > 0$ is the time step size. We set the value u_{jk}^n the numerical approximation of $u(x_j, y_k, t_n)$ and we define $u_{jk}^0 = u_0(x_j, y_k),\ j = 0, \ldots, N,\ k = 0, \ldots, N$.

The first order conservative scheme can be expressed as

$$u_{jk}^{n+1} = \frac{\Delta t}{h^2} A_{j-\frac{1}{2},k}^n u_{j-1,k}^n + \frac{\Delta t}{h^2} B_{j,k-\frac{1}{2}}^n u_{j,k-1}^n + \left(1 - \frac{\Delta t}{h^2}\left(A_{j-\frac{1}{2},k}^n + B_{j,k-\frac{1}{2}}^n + A_{j+\frac{1}{2},k}^n + B_{j,k+\frac{1}{2}}^n\right)\right) u_{jk}^n + \frac{\Delta t}{h^2} B_{j,k+\frac{1}{2}}^n u_{j,k+1}^n + \frac{\Delta t}{h^2} A_{j+\frac{1}{2},k}^n u_{j+1,k}^n \tag{62}$$

$$A_{j+\frac{1}{2},k}^n = \frac{v\frac{1}{2}(u_{jk}^n + u_{j+1,k}^n)}{\sqrt{\left(\frac{u_{jk}^n + u_{j+1,k}^n}{2}\right)^2 + \frac{r^2}{h^2}\left((u_{j+1,k}^n - u_{jk}^n)^2 + \left(\frac{0.5(u_{j,k+1}^n + u_{j+1,k+1}^n) - 0.5(u_{j,k-1}^n + u_{j+1,k-1}^n)}{2}\right)^2\right) + \epsilon}} \tag{63}$$

and

$$B_{j,k+\frac{1}{2}}^n = \frac{v\frac{1}{2}(u_{jk}^n + u_{j,k+1}^n)}{\sqrt{\left(\frac{u_{jk}^n + u_{j,k+1}^n}{2}\right)^2 + \frac{r^2}{h^2}\left((u_{j,k+1}^n - u_{jk}^n)^2 + \left(\frac{0.5(u_{j+1,k}^n + u_{j+1,k+1}^n) - 0.5(u_{j-1,k}^n + u_{j-1,k+1}^n)}{2}\right)^2\right) + \epsilon}} \tag{64}$$

where $r = \frac{v}{c}$. From Theorem 1 this scheme is stable if Δt is constrained to the Courant–Friedrichs–Lewy condition

$$\frac{\Delta t}{h^2} \leqslant \frac{1}{4v} \tag{65}$$

Similarly as performed in the one-dimensional case, we can relax the parabolic stability restriction by using either a full implicit or semi-implicit Crank–Nicolson procedure.

The scheme based on the trapezoidal rule can be written as

$$L^{n+1}(u^{n+1})_{jk} = R^n(u^n)_{jk} \tag{66}$$

where L^{n+1} and R^n are operators acting on the vectors u^{n+1} and u^n, respectively, and are defined as

$$L^{n+1}(u^{n+1})_{jk} = -\frac{1}{2}\frac{\Delta t}{h^2}A^{n+1}_{j-\frac{1}{2},k}u^{n+1}_{j-1,k} - \frac{1}{2}\frac{\Delta t}{h^2}B^{n+1}_{j,k-\frac{1}{2}}u^{n+1}_{j,k-1} + \left(1 + \frac{1}{2}\frac{\Delta t}{h^2}\left(A^{n+1}_{j-\frac{1}{2},k} + B^{n+1}_{j,k-\frac{1}{2}} + A^{n+1}_{j+\frac{1}{2},k} + B^{n+1}_{j,k+\frac{1}{2}}\right)\right)u^{n+1}_{jk} - \frac{1}{2} \times \frac{\Delta t}{h^2}B^{n+1}_{j,k+\frac{1}{2}}u^{n+1}_{j,k+1} - \frac{1}{2}\frac{\Delta t}{h^2}A^{n+1}_{j+\frac{1}{2},k}u^{n+1}_{j+1,k} \tag{67}$$

$$R^n(u^n)_{jk} = \frac{1}{2}\frac{\Delta t}{h^2}A^{n}_{j-\frac{1}{2},k}u^{n}_{j-1,k} + \frac{1}{2}\frac{\Delta t}{h^2}B^{n}_{j,k-\frac{1}{2}}u^{n}_{j,k-1} + \left(1 - \frac{1}{2}\frac{\Delta t}{h^2}\left(A^{n}_{j-\frac{1}{2},k} + B^{n}_{j,k-\frac{1}{2}} + A^{n}_{j+\frac{1}{2},k} + B^{n}_{j,k+\frac{1}{2}}\right)\right)u^{n}_{jk} + \frac{1}{2}\frac{\Delta t}{h^2}B^{n}_{j,k+\frac{1}{2}}u^{n}_{j,k+1} + \frac{1}{2} \times \frac{\Delta t}{h^2}A^{n}_{j+\frac{1}{2},k}u^{n}_{j+1,k} \tag{68}$$

The scheme (66) is fully implicit Crank–Nicolson. A semi-implicit version can be formulated as

$$L^{n}(u^{n+1})_{jk} = R^n(u^n)_{jk} \tag{69}$$

Both schemes are second order accurate in space and time and consist of solving Eqs. (66) or (69) at every time step. The same remarks stated for the one-dimensional case apply for this case. The semi-implicit scheme is recommended due to the obvious computational advantages concerning cost.

5. Numerical experiments

In this section we present numerical approximations to the relativistic heat equation for a set of different problems. We present first, third and fifth order accurate approximations of the solution using different initial data under homogeneous Neumann boundary conditions. The results of the proposed scheme and its high order accurate versions show good behavior according to the analytic properties examined above. Numerical results indicate that the algorithms behave stably and accurate, resolving sharply jump discontinuities (diffusion fronts) with correct speed of propagation.

Let $\bar{u}$ represent a high order accurate approximation of u. High order accuracy in space is obtained combining the basic solver as the proposed explicit conservative scheme or the semi-implicit Crank–Nicolson scheme together with a high order accurate reconstruction procedure. This is done dimension by dimension by means of the high order accurate reconstruction procedures applied to the conserved variable and its partial divided differences present in each coefficient of the nonlinear convex combination defining the scheme. A way to implement a high order accurate reconstruction procedure consists of determining an elementary function R_j at each computational cell $I_j = \left[x_{j-\frac{1}{2}}, x_{j+\frac{1}{2}}\right]$ of length $h > 0$ such that the mean value of R_j in the cell is the given data

$$u_j = \frac{1}{h}\int_{x_{j-\frac{1}{2}}}^{x_{j+\frac{1}{2}}} R_j(z)dz \tag{70}$$

and approximates the variable up to some order of accuracy in the cell [30]. We then obtain high accurate values of u at both sides of the interface $x_{j+\frac{1}{2}}$ as

$$\bar{u}^+_{j+\frac{1}{2}} = R_j(x_{j+\frac{h}{2}}) \tag{71}$$

and

$$\bar{u}^-_{j+\frac{1}{2}} = R_{j+1}(x_{j+\frac{h}{2}}) \tag{72}$$

The high order accurate value of the first derivative of u at the interface $x_{j+\frac{1}{2}}$ is obtained by calculating a function $S_j : [x_j, x_{j+1}] \to R$ such that

$$\frac{u_{j+1} - u_j}{h} = \frac{1}{h}\int_{x_{j-\frac{1}{2}}}^{x_{j+\frac{1}{2}}} S_j(z)dz \tag{73}$$

Then the approximation of u_x at $x_{j+\frac{1}{2}}$ is

$$(\bar{u}_x)_{j+\frac{1}{2}} = S_j(x_{j+\frac{h}{2}}) \tag{74}$$

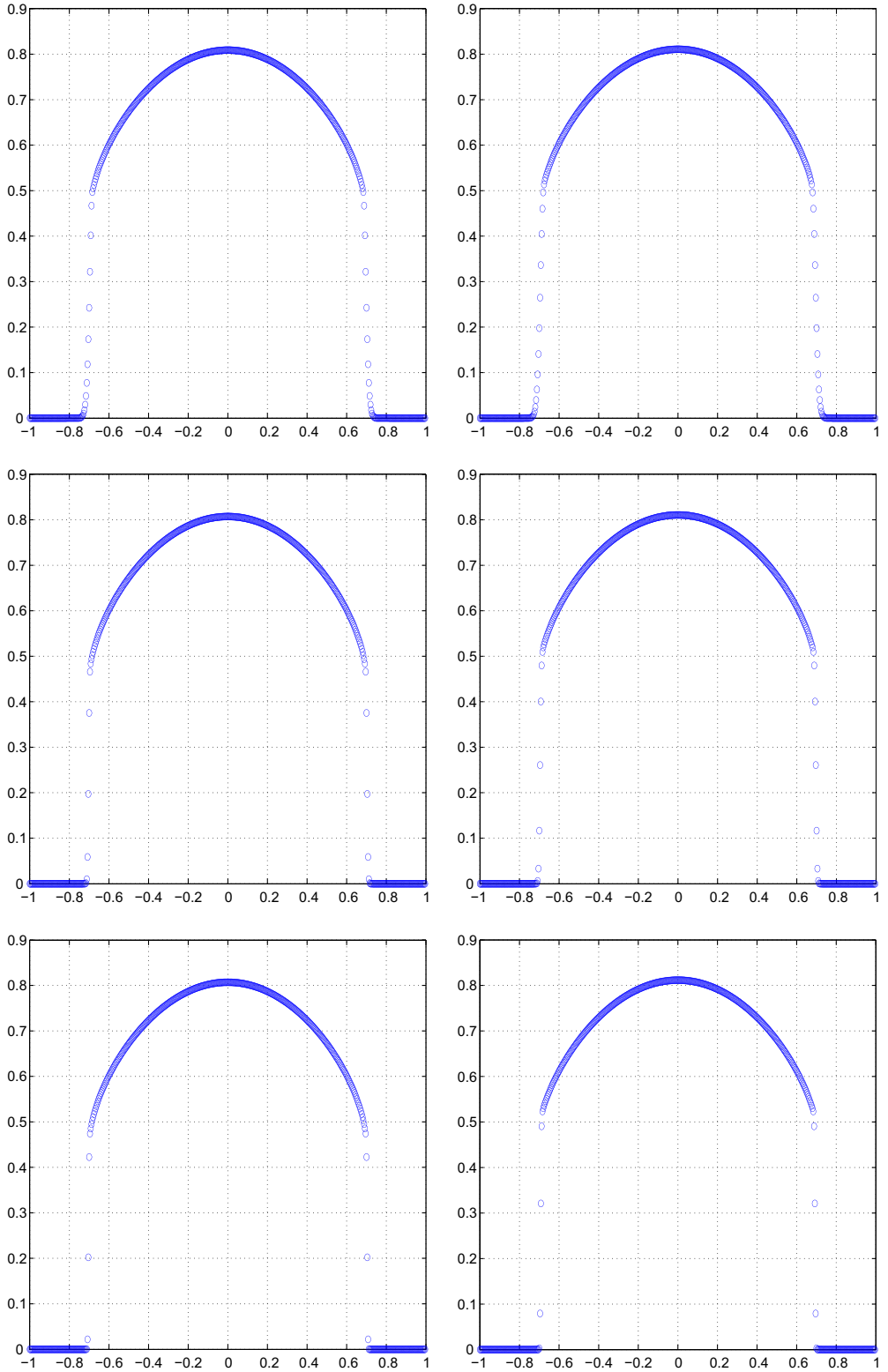

Fig. 1. Example 1: Results at time $t = 0.2$, $c = 1$, $v = 1$, $\epsilon = 1 \cdot e - 12$. Left column, explicit conservative scheme. Right column, semi-implicit Crank–Nicolson. Top to bottom, first order EC-1 and CN-1, third order EC-PHM-RK3 and CN-PHM-RK3 and fifth order EC-WPowerENO-RK3 and CN-WPowerENO-RK3 approximations.

Therefore the high order accurate value of $A(u_j, u_{j+1})$, (57) will be

$$\overline{A}_{j+\frac{1}{2}} = \frac{\frac{v}{2}(\bar{u}^-_{j+\frac{1}{2}} + \bar{u}^+_{j+\frac{1}{2}})}{\sqrt{\left(\frac{\bar{u}^-_{j+\frac{1}{2}} + \bar{u}^+_{j+\frac{1}{2}}}{2}\right)^2 + r^2(\bar{u}_x)^2_{j+\frac{1}{2}}}} \tag{75}$$

For the two-dimensional case, we use the one-dimensional procedure in each direction.

As reconstruction procedures we implement the third order accurate piecewise hyperbolic method (PHM) [23,29] that uses hyperbolas as elementary functions and the fifth order accurate Weighted PowerENO (WPowerENO) method [28] that is based on convex combinations of parabolas. The main advantage of using high order accuracy is that shock discontinuities are obtained sharper as higher is the order of the reconstruction procedure. Since the goal of our numerical experiments is to capture emerging shocks we will preferable use the fifth order version of the scheme to resolve them sharply.

The last step in the high order implementation is to achieve high order accuracy in time. For that purpose we use a third order accurate strong stability preserving Runge–Kutta method (RK3) [30,31].

The notation we will use to refer to the different schemes and orders of accuracy are as follows. For the basic solvers, we denote EC for the proposed explicit conservative scheme, and CN for the semi-implicit Crank–Nicolson scheme. We then add the corresponding labels for the order of accuracy being 1 for first order, PHM for third order and WPowerENO for fifth order. The last label to add will correspond to the Runge–Kutta method for the cases where high order accuracy is used.

5.1. Example 1: Square wave problem

In this experiment we approximate the solution of the one-dimensional relativistic heat equation, Eq. (53) with $c = 1$ and $v = 1$, for the "square wave" initial data

$$u_0(x) = \begin{cases} 1; & -\frac{1}{2} \leqslant x \leqslant \frac{1}{2} \\ 0; & \text{elsewhere} \end{cases}$$

in $x \in [-1, 1]$ under homogeneous Neumann boundary conditions.

We compute until time $t = 0.2$ with a grid of 500 points. We run the conservative numerical scheme (explicit) 25,000 iterations with $\Delta t = 0.5h^2$ and $\epsilon = 1 \cdot e - 12$ and the semi-implicit Crank–Nicolson scheme 800 iterations with $\Delta t = \frac{1}{16}h$.

Left column in Fig. 1 displays the numerical approximation obtained with the explicit conservative scheme for different order approximations: first (EC-1), third (EC-PHM-RK3) and fifth order (EC-WPowerENO-RK3), top to bottom, respectively. Right column displays the corresponding numerical approximations(results) computed with the semi-implicit Crank–Nicolson scheme with first (CN-1), third (CN-PHM-RK3) and fifth (CN-WPowerENO-RK3) order accuracy, respectively.

We observe that the first order explicit and semi-implicit schemes perform stable and accurate and jump discontinuities are propagated at correct speed. High order versions of the respective schemes behave similarly with sharper resolution in jump discontinuities. The advantage of the semi-implicit scheme with respect to the explicit ones relies on the speed up of the computational cost.

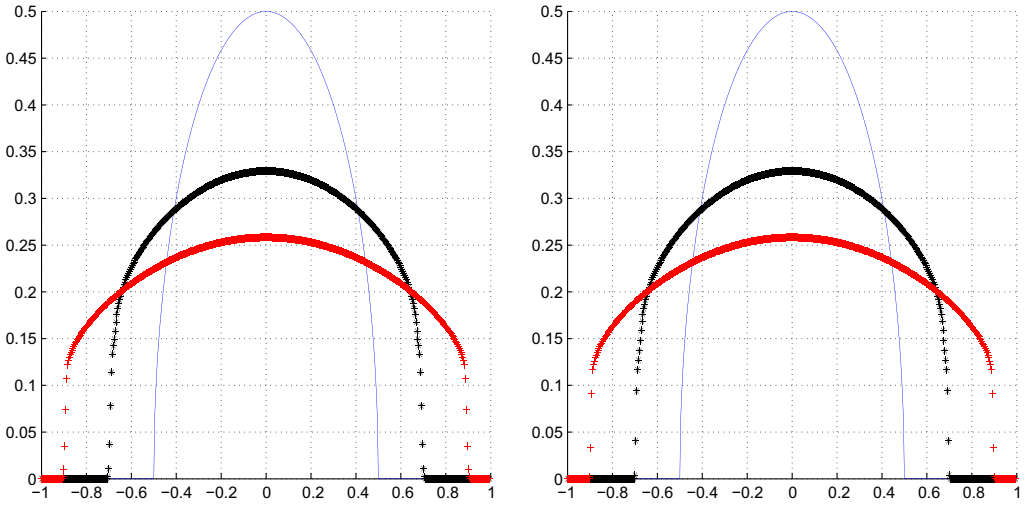

Fig. 2. Example 2: Explicit conservative EC-PHM-RK3 (left) and EC-WPowerENO5-RK3 (right) approximations at times $t = 0.2$ ("$*$") and $t = 0.4$ ("+") versus initial data ("$-$").

5.2. Example 2: Semi-circle wave problem

We consider the one-dimensional relativistic heat equation Eq. (53) with $c = 1,\ v = 1$. The initial data is a semi-circle defined in $x \in [-1, 1]$ by

$$u_0(x) = \begin{cases} \sqrt{0.25 - x^2}; & -\frac{1}{2} \leqslant x \leqslant \frac{1}{2} \\ 0; & \text{elsewhere} \end{cases}$$

with homogeneous Neumann boundary conditions. This is a case of a continuous initial data with compact support such that the slopes at both ends of the support are vertical. This example shows numerical evidence that the solution of the relativistic heat equation with a continuous function as initial data might develop diffusion fronts at finite time.

We compute the approximate solution at times $t = 0.2$ and $t = 0.4$ with a uniform grid of 500 points. We run the explicit conservative scheme with $\Delta t = 0.5 * h^2$. In Fig. 2 we display the numerical approximation of the solution at both times $t = 0.2$ represented with "$*$" and $t = 0.4$ with "+". In the left are the results computed with the explicit conservative third order accurate scheme (EC-PHM-RK3) and in the right the ones with the fifth order accurate version (EC-WPowerENO-RK3).

The results show that both calculations capture jump discontinuities evolving to the right and to the left with speed $c = 1$. These are diffusion fronts formed at finite time. We observe that the resolution of the jump discontinuities is sharper for the fifth order accurate case.

5.3. Example 3: Initial double wave problem

We consider the one-dimensional relativistic heat equation Eq. (53) with $c = 1,\ v = 1$, and an initial data in $x \in [-1, 1]$ consisting on two "square waves" with disjoint supports located at a positive distance. This initial data is defined by

$$u_0(x) = \begin{cases} 0.6; & -\frac{1}{2} \leqslant x \leqslant -\frac{1}{4} \\ 0.8; & \frac{1}{4} \leqslant x \leqslant \frac{1}{2} \\ 0; & \text{elsewhere} \end{cases}$$

with homogeneous Neumann boundary conditions.

We compute the approximation of the solution at times $t = 0.2$ and $t = 0.4$ using a uniform grid of 500 points. The numerical approximations at time $t = 0.2$ maintains the two waves with disconnected supports. At time $t = 0.4$ the supports merge into one which is connected and the interior fronts disappear.

We run the explicit conservative scheme with $\Delta t = 0.5 * h^2$. Fig. 3 displays the numerical approximation of the solution at both times $t = 0.2$ and $t = 0.4$ represented with "$*$" and"+", respectively. Left picture includes the results with the explicit conservative third order accurate scheme (EC-PHM-RK3) and the right one the results with the explicit conservative fifth order accurate scheme (EC-WPowerENO-RK3). Both schemes behave stable and accurate and propagate jump discontinuities at correct speed.

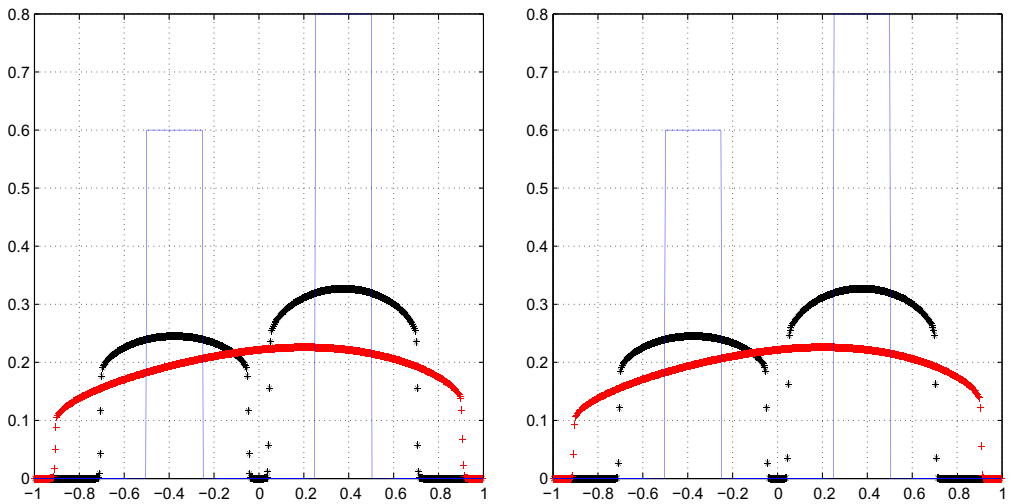

Fig. 3. Example 3: Explicit conservative EC-PHM-RK3 (left) and EC-WPowerENO5-RK3 (right) approximations at times $t = 0.2$ ("$*$") and $t = 0.4$ ("+") versus initial data ("$-$").

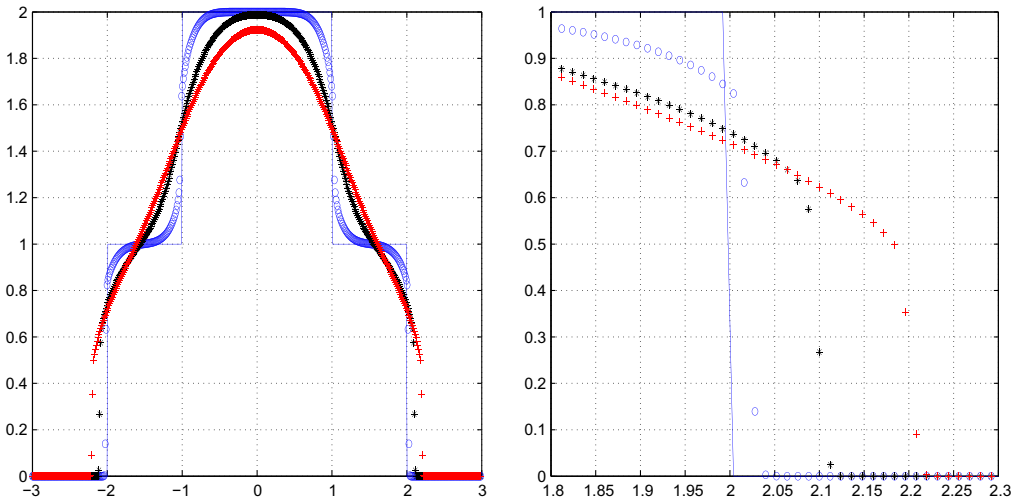

Fig. 4. Example 4: Left, explicit conservative fifth order EC-WPowerENO-RK3 approximations at times $t = 0.025$ ("$\circ$"), $t = 0.1$ ("$*$") and $t = 0.2$ ("+") versus initial data ("$-$"). Right, zoomed region of the left picture.

5.4. Example 4: Double step problem

We consider the initial-boundary value problem with the one-dimensional relativistic heat equation under homogeneous Neumann boundary conditions and the compactly supported initial data

$$u_0(x) = \begin{cases} 2; & |x| \leqslant 1 \\ 1; & -2 \leqslant x < -1 \\ 1; & 1 \leqslant x \leqslant 2 \\ 0; & \text{elsewhere} \end{cases}$$

defined in $x \in [-3, 3]$.

In this linear combination of characteristic functions the discontinuities are initially located at $x = \pm 1$ and $x = \pm 2$. The expected evolution of this initial predicts that discontinuities at $x = \pm 1$ disappear in finite time since the diffusion coefficient around $x = \pm 1$ is proportional to u^3 and that diffusion fronts located initially at $x = \pm 2$ survive and propagate at finite speed $(c = 1)$ expanding the support of the evolving signal.

We compute the approximate solution with a uniform grid of 500 grid points using the fifth order version of the proposed explicit conservative scheme, EC-WPowerENO5-RK3, with $\Delta t = 0.5h^2$. Left picture in Fig. 4 displays the numerical approxi-

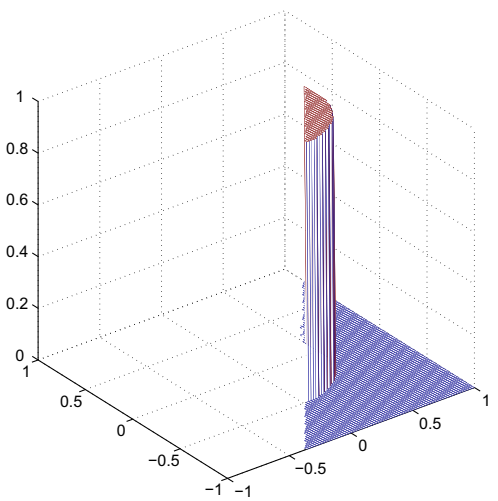

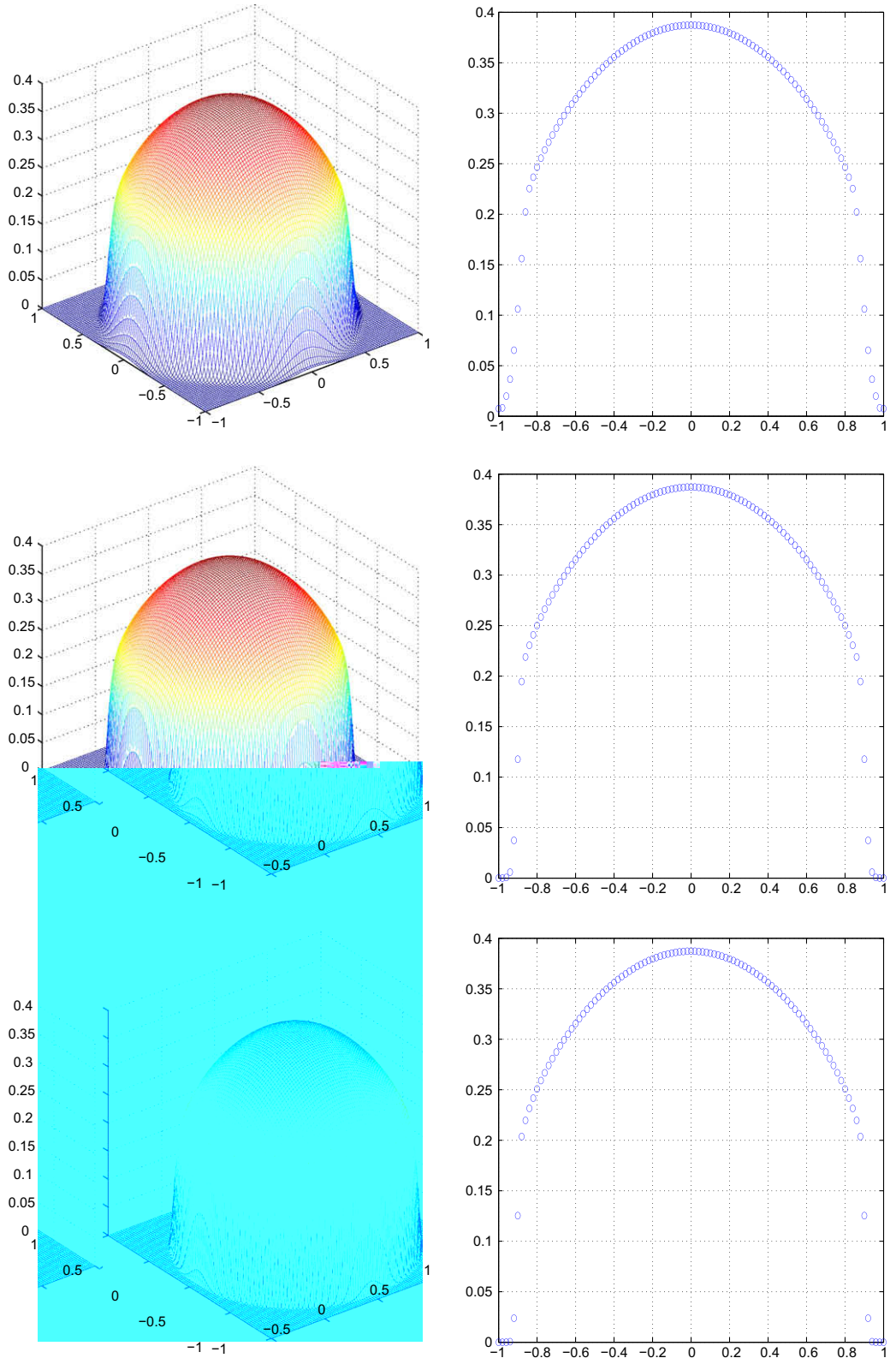

Fig. 6. Example 5: Results at time $t = 0.4$ versus x-sections. Top to bottom: first order EC-1, third order EC-PHM-RK3 and fifth order EC-WPowerENO-RK3 approximations.

mation of the solution computed at times $t = 0.025$, $t = 0.1$ and $t = 0.2$ represented by "$\circ$", "$*$" and"+", respectively. We observe that initial discontinuities at $x \pm 1$ disappear at short time and diffusion fronts remain jump discontinuities that propagate at correct speed. Diffusion fronts are resolved sharp for the high order accurate approximations. Right picture in Fig. 4 shows zoomed regions of left picture around the right diffusion front. We observe that the discontinuity front has a vertical contact angle as predicted in the analytical results presented in [5].

5.5. Example 5: Disc problem

We consider the two-dimensional relativistic heat Eq. (59) with $c = 1$ and $v = 1$. The initial data displayed in Fig. 5 consists of the characteristic function of a disc of height 1 and radius 0.5 centered in the domain $D = [-1,1] \times [-1,1]$. The initial diffusion front is a jump discontinuity at the boundary of the support of the function. The evolution of this data through the relativistic heat equation spreads out the diffusion front with constant velocity in the outward direction preserving the shape of a circle which radius at time $t > 0$ will be $r(t) = 0.5 + t$ since $c = 1$. We have computed the approximate solution of the relativistic heat equation at time $t = 0.4$ using a uniform grid of 100×100 grid points in D. We use the explicit conservative scheme with a time step $\Delta t = 0.25h^2$ where $h = 0.02$. Left column in Fig. 6 displays, from top to bottom, the numerical solution for the first EC-1, third EC-PHM-RK3 and fifth EC-WPowerENO5-RK3 order accurate schemes, respectively. In the right column in same figure we depict the corresponding central x-section of the numerical solutions in left column.

5.6. Example 6: Relativistic porous media equation

We consider a one-dimensional initial-boundary value problem for the following generalization of the relativistic heat equation that can be considered a porous media type equation

$$u_t = v\left(\frac{u^m u_x}{\sqrt{u^2 + r^2 u_x^2}}\right)_x \tag{76}$$

with $m > 1$. The initial data we assume is defined in $[-2,2]$ as

$$u_0(x) = \max(1 - x^2, 0) \tag{77}$$

under homogeneous Neumann boundary conditions. The goal of this experiment consists in observing that the initial signal, which is continuous, develops jump discontinuities at the boundaries of the support in finite time. We can observe two different phases in the evolution. The first stage corresponds to the growth of the slope of the contact angle until it becomes vertical and the second begins when the discontinuity breaks and starts propagating with finite speed expanding the support.

In our calculations we set $m = 2$ and use a uniform grid of 500 points and $\Delta t = 0.5 * h^2$ where $h = \frac{4}{500}$. We compute the approximate solution with the fifth order accurate version of the explicit conservative scheme EC-WPowerENO5-RK3 at times $t = 0.1$, 0.2 and 0.4 represented in the left picture of Fig. 7 with "$\circ$", "$*$" and"+", respectively. We observe that around time $t = 0.2$ the contact angle becomes vertical and fronts start evolving with finite speed. Right picture of the figure shows

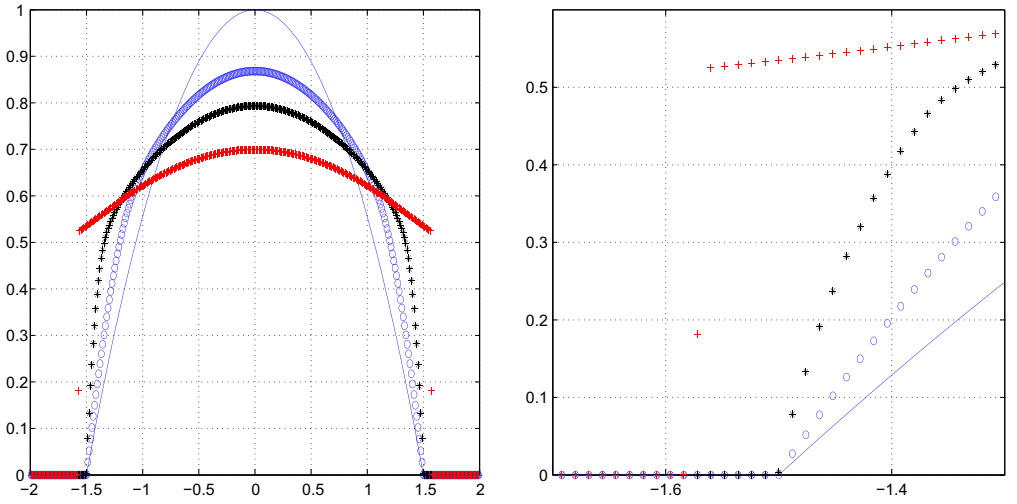

Fig. 7. Example 6: Left, explicit conservative fifth order EC-WPowerENO-RK3 approximations at times $t = 0.1$ ("$\circ$"), $t = 0.2$ ("$*$") and $t = 0.4$ ("+") versus initial data ("$-$"). Right, zoomed region of the left picture.

the zoomed left angle region were we observe the growing of the slope of the contact angle at different times of the evolution.

The numerical results presented in this section indicate that the proposed scheme is robust, behaves stably and captures sharply diffusion fronts with a correct speed of propagation. The results are in accordance with the mathematical theory developed by Andreu and collaborators in [1,2,4,5].

6. Conclusions

We have proposed a conservative finite difference numerical scheme to approximate the solution of initial-boundary value problems for a class of limited diffusion Fokker–Planck equations under homogeneous Neumann boundary conditions. We have proved that the numerical scheme preserves positivity, satisfies a discrete local maximum principle and is stable under a Courant–Friedrichs–Lewy time step restriction. We have analyzed the dynamics of the relativistic heat equation as a model example of the generalized class of Fokker–Planck equations and presented numerical experiments in one and two dimensions showing the presence of diffusion fronts that propagate with finite velocity for the case where the initial data is continuous.

Acknowledgment

This work is supported by grant DGICYT MTM2008-03597.

References

[1] F. Andreu, V. Caselles, J.M. Mazon, A strongly degenerate quasilinear elliptic equation, Nonlinear Anal. 61 (2005) 637–669.
[2] F. Andreu, V. Caselles, J.M. Mazon, The Cauchy problem for a strongly degenerate quasilinear equation, J. Eur. Math. Soc. 7 (2005) 361–393.
[3] F. Andreu, V. Caselles, J.M. Mazon, S. Moll, Finite propagation speed for limited flux diffusion equation, Arch. Ration. Mech. Anal. 182 (2006) 269–297.
[4] F. Andreu, V. Caselles, J.M. Mazon, S. Moll, A diffusion equation in transparent media, J. Evol. Equat. 7 (2007) 113–143.
[5] F. Andreu, V. Caselles, J.M. Mazon, Some regularity results on the relativistic heat equation, J. Differ. Equat. 245 (2008) 3639–3663.
[6] F. Bampi, A. Morro, Relativistic heat equation in casual nonstationary thermodynamics, Phys. Lett. 79A (2/3) (1980) 156–158.
[7] G.I. Barenblatt, On some unsteady motions of a liquid or a gas in a porous media, Prikl. Mat. MEch. 16 (1952) 67–78.
[8] Y. Brenier, Extended Monge–Kantorovich theory, in: Optimal Transportation and Applications: Lectures given at the CIME Summer School held in Martina Franca, Lectures Notes in Mathematics, vol. 1813, Springer-Verlag, 2003, pp. 91–122.
[9] V. Caselles, Convergence of the relativistic heat equation to the heat equation as $c \to \infty$, Publ. Mat. 51 (2007) 121–142.
[10] C. Cattaneo, Sulla conduzione del calore Atti. del Semin. Matem., Unive di Modena, vol. 3, 1948–1949, pp. 83–101.
[11] A. Chertock, A. Kurganov, P. Rosenau, Formation of discontinuities in flux-saturated degenerate parabolic equations, Nonlinearity 16 (2003) 1875–1898.
[12] R. Courant, K. Friedrichs, H. Lewy, Partial differential equations of mathematical physics, Math. Ann. 100 (1928) 32–74.
[13] M.G. Crandall, H. Ishii, P.L. Lions, Users guide to viscosity solutions of 2-nd order partial differential equations, Bull. Am. Math. Soc. 27 (1) (1992) 1–67.
[14] J. Crank, P. Nicolson, A practical method for numerical evaluation of solution of partial differential equations of the heat conduction type, Proc. Camb. Philos. Soc. 43 (1947).
[15] J.J. Duderstadt, G.A. Moses, Inertial Confinement Fusion, John Wiley and Sons, 1982.
[16] J. Fourier, Theorie analytique de la chaleur (1822).
[17] Y. Giga, Viscosity solutions with shocks, Commun. Pure Appl. Math. LV (2002) 0431–0480.
[18] A.C. Gurtin, M.E. Pipkin, A general theory of heat conduction with finite wave speeds, Arch. Ration. Mech. Anal. 31 (1968) 113–126.
[19] R. Jordan, D. Kinderlehrer, F. Otto, The variational formulation of the Fokker–Planck equation, SIAM J. Math. Anal. 29 (1) (1998) 1–17.
[20] D. Joseph, L. Preziosi, Heat waves, Rev. Mod. Phys. (1989) 41–73.
[21] P. Lax, B. Wendroff, Systems of conservation laws, Commun. Pure Appl. Math. 13 (2) (1960) 217–237.
[22] H. Levine, M.P. McGee, S. Serna, Diffusion and reaction in the cell glycocalyx and the extracellular matrix, J. Math. Biol. 60 (1) (2010) 1–26.
[23] A. Marquina, Local piecewise hyperbolic reconstruction of numerical fluxes for nonlinear scalar conservation laws, SIAM J. Sci. Comput. 15 (4) (1994) 892–915.
[24] R. Metzler, J. Klafter, The random walk's guide to anomalous diffusion: a fractional dynamics approach, Phys. Rep. Rev. Sec. Phys. Lett. 339 (1) (2000) 1–77.
[25] D. Mihalas, B. Mihalas, Foundations of Radiation Hydrodynamics, Oxford University Press, Oxford, 1984.
[26] P. Rosenau, Tempered diffusion: a transport process with propagation front and inertial delay, Phys. Rev. A 46 (1992) 7371–7374.
[27] L. Rudin, S. Osher, E. Fatemi, Nonlinear total variation base noise removal algorithms, Physica D 60 (1–4) (1992) 259–268.
[28] S. Serna, A. Marquina, Power ENO methods: a fifth-order accurate weighted power ENO method, J. Comput. Phys. 194 (2) (2004) 632–658.
[29] S. Serna, A class of extended limiters applied to piecewise hyperbolic methods, SIAM J. Sci. Comput. 28 (1) (2006) 123–140.
[30] C.W. Shu, S. Osher, Efficient implementation of essentially non-oscillatory shock-capturing schemes, 2, J. Comput. Phys. 83 (1) (1989) 32–78.
[31] R.J. Spiteri, S.J. Ruuth, A new class of optimal high-order strong-stability-preserving time discretization methods, SIAM Numer. Anal. 40 (2) (2002) 469–491.
[32] C. Tsallis, D.J. Bukman, Anomalous diffusion in the presence of external forces: exact time-dependent solutions and their thermostatistical basis, Phys. Rev. E 54 (3) (1996) R2197–R2200.
[33] D.M. Young, Iterative Solution of Large Linear Systems, Academic Press, New York, 1971.
[34] M. Zakari, D. Jou, A generalized Einstein relation for flux-limited diffusion, Physica A 253 (1998) 205–210.
[35] M. Zakari, A continued-fraction expansion for flux limiters, Physica A 240 (1997) 676–684.